Transient structural response to photoexcitation in polyacetylene

E. J. Mele
Department of Physics, Laboratory for Research on the Structure of Matter, University of Pennsylvania, Philadelphia, Pennsylvania 19104-3859
(Received 6 July 1982)

An equation-of-motion procedure to study intramolecular vibrational relaxation in polyatomic molecules is developed and applied to study the transient structural response of a polyene to photoexcitation. The lattice response at short times (~ 20 fs) following excitation is characterized by an adiabatic relaxation which is highly specific to the exciting frequency. For longer times (20–1000 fs) this relaxation is strongly modified by the nonadiabatic relaxation of the excited carrier and takes the form of a "splash" in the bond-alternation profile, which reflects the transient distribution of the excited carrier in energy.

Recent interest in polyacetylene has largely been focused on the interesting electrical properties of this material[1–3] (a doping-induced insulator-metal "transition,"[1,2] having potential use as a battery electrode[3]) and the consideration of $(CH)_x$ as a medium which supports nonlinear structural excitations, or solitons.[4,5] Considerable evidence has been presented to demonstrate the importance of solitons in the charge-transfer doping of this polymer,[6–10] and it has further been suggested that such defects also occur in response to the creation of electron-hole pairs by photoexcitation.[11] This theoretical suggestion is supported by a Born-Oppenheimer calculation of the structural response of a model polyene to the creation of an electron-hole pair at the band edges. We have generalized such a computational procedure to include possible nonadiabatic processes, i.e., transitions between excited electronic states, and have applied it to study the transient structural response of a polyene when carriers are created above the band edge which is the more frequently experimentally realized situation in $(CH)_x$.[12–16] In this study we obtain a number of interesting new dynamic phenomena which are dominantly attributable to the nonadiabatic relaxation channel. Among these are the evolution of a "splash" or localized modulation of the bond-alternation profile as the carriers relax towards the band edges; these dynamic structural configurations directly reflect the transient distribution of the excited carrier in energy. A more detailed account of our computational procedure is planned to be forthcoming; in the present paper we will briefly outline the computational method and discuss several specific results for the relaxation in $(CH)_x$. Of immediate experimental interest, we find that spectral line shapes for secondary photons emitted by radiative recombination of the electron and hole during this relaxation provide a strikingly good description of the unusual Stokes-shifted lines reported in $(CH)_x$ and routinely attributed to an inhomogeneous distribution of conjugated lengths in the material.[12,14] Furthermore, while the adiabatic gemination of solitons following band-edge excitation is extremely fast[11] (~ 20 fs) the formation of such defects following photoexcitation above the band gap is significantly slower, being limited by the transit time of the carrier to the band edge (~ 1 ps). This time domain is presently experimentally accessible, suggesting that the gemination of photoexcited defects in the polyene may be directly experimentally monitored in time.

To describe the coupled electron-lattice system in $(CH)_x$ we adopt the parametrized Hückel Hamiltonian[5,17]:

$$H=\sum_{n,\sigma}(t_n c^{\dagger}_{n+1,\sigma}c_{n,\sigma}+t_{n-1}c^{\dagger}_{n-1,\sigma}c_{n,\sigma}) +\tfrac{1}{2}K\sum_n (u_{n+1}-u_n)^2 +\sum_n[M\dot{u}_n^2-\Gamma(u_{n+1}-u_n)]\,, \tag{1}$$

where $c_{n,\sigma}$ annihilates a π electron of spin σ on site n, u_n labels the longitudinal displacement of each carbon atom from its location in the equal-bond-length structure, and M is the ion mass. The hopping integrals in Eq. (1), $\{t_n\}$, are linearized in the u_n:

$$t_n=t_0+\alpha(u_{n+1}-u_n)\,, \tag{2}$$

and $\Gamma=4(\alpha/\pi)$. Taking $t_0=-3.0$ eV, $K=68.6$ eV Å^{-2}, and $\alpha=8.0$ eV Å^{-2}, one obtains a 12-eV bandwidth, a 1.4-eV band gap, and an equilibrium dimerization amplitude $|u_n|=0.023$ Å in the ground state, results which are representative of *trans*-$(CH)_x$.[17]

To investigate the polyene dynamics in the photoexcited state, we wish to calculate the time evolution of the ion coordinates $\{u_n\}$ in response to a time-dependent force from the occupied electronic states. We summarize the computational method as follows.[18] We first diagonalize the electronic part of Eq. (1) for some structural configuration $\{u_n\}$,

$$H_e[u_n]\psi_\alpha=E_\alpha\psi_\alpha \ , \tag{3}$$

and construct the density operator from the resulting eigenstates $\{\psi_\alpha\}$:

$$\hat{\rho}=\sum_\alpha f_\alpha\psi_\alpha^\dagger\psi_\alpha \ , \tag{4}$$

where f_α are the occupation numbers for the states, α. This density exerts a force on the nth ion coordinate:

$$F_n=-\frac{\partial}{\partial u_n}\sum_\alpha f_\alpha E_\alpha \ , \tag{5}$$

which is to be combined with the lattice part of Eq. (1) to yield a classical equation of motion for the u_n:

$$M\ddot{u}_n=K(u_{n+1}+u_{n-1}-2u_n)-\gamma\dot{u}_n+F_n \ . \tag{6}$$

In Eq. (3) we recognize two origins of the classical driving force F_n. First, the adiabatic modulation of the eigenvalues, E_α, produces an adiabatic force,

$$F_n^{(a)}=-\sum_\alpha f_\alpha\frac{\partial E_\alpha}{\partial u_n} \ , \tag{7a}$$

$$F_n^{(a)}=-\sum_\alpha \rho_{\alpha\alpha}[H^n_{e\text{-ph}}]_{\alpha\alpha} \ , \tag{7b}$$

where we define the deformation potential

$$[H^n_{e\text{-ph}}]_{\alpha\alpha}=\left\langle\psi_\alpha\left|\frac{\partial H_e}{\partial u_n}\right|\psi_\alpha\right\rangle \ .$$

Second, transitions between electronic levels induced by the ion motion produces an additional nonadiabatic term,

$$F_n^{(\mathrm{na})}=-\sum_\alpha\frac{\partial\rho_{\alpha\alpha}}{\partial u_n}[H_e]_{\alpha\alpha} \ . \tag{8a}$$

A perturbation expansion yields

$$\frac{\partial\rho_{\alpha\alpha}}{\partial u_n}=\sum_{\beta\neq\alpha}\left[\frac{[H^n_{e\text{-ph}}]_{\alpha\beta}}{E_\alpha-E_\beta}\rho_{\alpha\beta}+\frac{[H^n_{e\text{-ph}}]^*_{\alpha\beta}}{E_\alpha-E_\beta}\rho_{\beta\alpha}\right] , \tag{8b}$$

where $\rho_{\beta\alpha}$ denote off-diagonal terms in the density matrix which are, in general, nonzero for a system evolving in time from the starting configuration in Eq. (4). By combining the $\alpha\beta$ and $\beta\alpha$ terms in the resulting double sum in Eq. (8), we obtain

$$F_n^{(\mathrm{na})}=-\sum_{\alpha,\beta}{}'\rho_{\alpha\beta}[H^n_{e\text{-ph}}]_{\beta\alpha} \ , \tag{9}$$

where the prime excludes the $\alpha=\beta$ term in the summation. The matrix $\hat{\rho}$ thus will completely specify the instantaneous electronic force exerted on the ions. The $\hat{\rho}$ also evolve in time according to

$$\frac{\partial\hat{\rho}}{\partial t}=\frac{-i}{\hbar}[H[u],\hat{\rho}]+\left.\frac{\partial\hat{\rho}}{\partial t}\right|_{\text{damping}} \ , \tag{10}$$

where H depends on the u_n following the linearized dependence given in Eq. (2). The damping term includes the effect of interactions not specifically included in the Hamiltonian in Eq. (1),[18,19] which are assumed to be stochastic in nature and which will consequently exponentially reduce the off-diagonal terms in $\hat{\rho}$ if the polyene is left in a fixed configuration $\{u_n\}$.

A complete solution for the polyene dynamics thus requires the parallel integration of the equations of motion (6) and (10) for the ion coordinates and density matrix, respectively. In practice this may be difficult because some of the terms in $\hat{\rho}$ oscillate much faster than the ion coordinates, imposing an inefficiently fine integration mesh on the problem. In our approach to this problem we seek to integrate both sets of equations on a mesh which is designed to accurately describe the ion motions. For the electronic degrees of freedom we construct a piecewise continuous solution for the time evolution of the density matrix on the same "coarse" mesh. In each time increment $(t,t+\Delta t)$ we propagate the electronic states as though the ion coordinates were frozen in the configuration $\{u_n(t)\}$. The characteristic solutions to Eq. (8) are then

$$\hat{\rho}_{\alpha\beta}(t)=\psi_\alpha^\dagger\psi_\beta\exp[-i(E_\alpha-E_\beta)t] \times\exp[-(1-\delta_{\alpha\beta})\Gamma_{\alpha\beta}t] \ , \tag{11}$$

where, as previously $H_e[u_n(t)]\psi_\alpha=E_\alpha\psi_\alpha$. To complete the piecewise integration of Eq. (8) we require a boundary condition for $u_n(t)$ in each such interval. This is provided by transforming $\hat{\rho}$ into the site representation $\{|i\rangle\}$ and demanding that the $\langle i|\rho|j\rangle$, which represent the physical charge density, remain continuous upon crossing between two adjacent intervals. Thus returning to the representation of "instantaneous" eigenstates, we have

$$\hat{\rho}(t+\Delta t)=O^{\dagger}\sum_{\alpha\beta}\rho_{\alpha\beta}\exp[-i(E_{\alpha}-E_{\beta})\Delta t]O\ , \tag{12}$$

where

$$O_{\alpha\beta}=\langle\psi_{\alpha}(t+\Delta t)\,|\,\psi_{\beta}(t)\rangle\ . \tag{13}$$

With this scheme, the electronic degrees of freedom can be efficiently propagated on the same integration mesh as required for a description of the ion motions. Notice that if the energy difference between two states α and β in the electronic manifold is large compared to a phonon frequency, the associated term $\rho_{\alpha\beta}$ in the density matrix oscillates rapidly on the scale of a phonon period and energy transfer from such an electronic oscillator to the lattice is inhibited. Conversely, if the energy difference between states α and β is well matched to a phonon frequency, the nonadiabatic force in Eq. (7) acts coherently with the ion response to efficiently deliver energy into the lattice. The evolution of the $\rho_{\alpha\beta}$ described by Eqs. (10)–(13) thus naturally builds into the problem constraints imposed by energy conservation and the selection rules governed by the symmetry of the electronic and vibrational states coupled by Eq. (1). Notice that this is accomplished without having to reference a specific set of adiabatic vibrational normal modes which are prohibitively difficult to evaluate and would at any rate yield a poor approximation to the actual time evolution of the lattice displacements. The evolution of the diagonal elements in $\hat{\rho}$ provides information about the transient decay of the excited carrier in energy and the parallel evolution of the atomic coordinates provides information about the distribution of phonons involved in the relaxation.

We now turn to consider the relaxation in polyacetylene following photoexcitation. The calculations described here are performed on a finite 48-atom chain. The equations of motion are integrated in time, each interval in the integration is 0.5 fs wide so that roughly 40 iterations are required to span an optical-phonon period. In the starting configuration the ion coordinates are fixed in the ground-state configuration and the density matrix, initially diagonal in the representation of energy eigenstates, describes the result of an optical excitation from state n to n':

$$\rho_{\alpha\alpha}=\begin{cases}2, & E_{\alpha}<E_{f},\ \ \alpha\neq n\\ 1, & \alpha=n\\ 1, & \alpha=n'\ .\end{cases} \tag{14}$$

The initial and final states n and n', connected in the absorption process are symmetrically positioned about the band gap as would be required by momentum conservation were the chain infinite. As we have noted in a previous Communication,[18] once the system is prepared in this excited configuration, the time required for a transition between electronic excited states is substantially longer than the time required for an adiabatic relaxation on the single excited state potential surface. Thus the short-time dynamics is dominated by the adiabatic force in Eq. (7). This is very significant because the deformation potentials defined in Eq. (7) are tremendously sensitive to the particular state n in which they are evaluated. For the mth electronic excitation above the optical threshold the $H^{n}_{e\text{-ph}}$ undergo a sinusoidal modulation as a function of position on the polyene which is well described away from the chain ends by

$$[H^{n}_{e\text{-ph}}]_{mm}\sim V\cos[2\pi nm/(N-1)]\ , \tag{15}$$

where N is the number of atoms in the chain. For example, the lattice configuration obtained a short time ($\sim 10^{-14}$) after photoexcitation in response to this adiabatic force is shown in Fig. 1 for the third, fifth, and seventh "allowed" optical excitations of the chain. This short-time lattice response clearly demonstrates this excitation-frequency dependence of the adiabatic driving force. This interesting behavior is most easily understood by considering the infinite-chain limit in which $[H^{n}_{e\text{-ph}}]_{mm}$ drives a lattice distortion which connects two degenerate states across the Brillouin zone with the energy of the final state involved in the absorption. In this limit, the adiabatic force apparently drives a Peierls-type distortion on the excited-state surface.

As the polymer continues to relax, amplitude for the excited electron grows in states closer to the band gap. In our semiclassical picture we find that

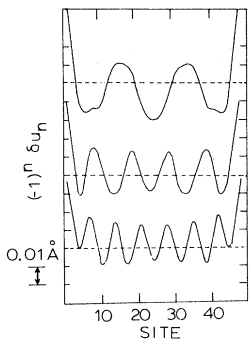

FIG. 1. Graphs of the distortions in the bond-alternation profile of a 48-atom polyene 10 fs following photoexcitation of the third, fifth, and seventh allowed optical excitations of the chain. The dashed line in each panel denotes the undistorted configuration.

the nonadiabatic force in Eq. (9) begins to drive the carbon motions, doing work on the ions and hence transferring energy from the electronic manifold to the lattice. From Eq. (9) the nonadiabatic contribution is completely attributable to the off-diagonal terms in $\hat{\rho}$ in the representation of energy eigenstates. Thus the energy transfer is most efficient for processes which involve the off-diagonal terms in $\hat{\rho}$ which are oscillating coherently with the lattice, i.e., well matched in frequency. Thus one recovers in this procedure a detailed picture in time of the transition of the excited electron between excited states.

Graphs of the lattice configuration are shown in Fig. 2 for times extending out to 100 fs following photoexcitation of the fifth allowed optical transition of the chain. To obtain these profiles we have removed a spatially rapidly oscillating part from these distortions by Fourier analyzing the real-space distortion and retaining the components with $q \leq 10(2\pi/L)$ where L is the chain length, in the back transform. These suppressed rapid oscillations

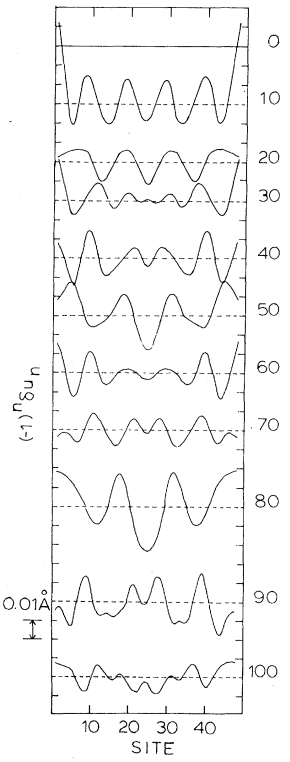

FIG. 2. Graphs of the distortions in the bond-alternation profile of a 48-atom polyene as a function of time following photoexcitation of the fifth allowed optical excitation of the chain. The dashed lines in each panel denote the undistorted configuration. The numbers in the right-hand column denote the elapsed time following the excitation in units of 10^{-15} s.

are of peripheral interest in the present study since they are dominantly due to an overall swelling of the chain which occurs in the excited state.

In Fig. 2 we observe that as time increases the dimerization profile undergoes a series of bounces; we can identify two dominant effects which occur with each successive bounce. First, it is apparent that the lattice distortion is becoming more and more pronounced at the center of the chain. Second, the sinusoidal modulations of the bond-alternation profile are evolving to longer wavelengths or smaller momenta, as time increases. If extended to much longer times, we will ultimately recover a lattice configuration containing two photogenerated solitons, in which there will be a reversal of the bond-alternation amplitude at the center of the chain without the modulated structure shown in Fig. 2. However, Fig. 2 demonstrates that the formation of such defects is a continuous process which begins while the carrier resides above the band edge. In fact, Fig. 2 describes a continuous localization of the excited carrier as it relaxes towards the band edge. The evolution of the sinusoidal modulation of the bond-alternation profile to longer wavelengths as the carrier relaxes is the result of an interesting interplay between the adiabatic and nonadiabatic relaxation channels. As the excited carrier relaxes, its amplitude in states closer to the band edge is continuously increasing. Crudely speaking the states closer to the band edge are the states which are adiabatically coupled to the longer-wavelength distortions of the lattice through Eq. (11). Qualitatively, we then expect the growth of a lattice distortion which is a superposition of sinusoidal modulations from the dynamically occupied states. Since the electron distribution is spreading in momenta, this implies the formation of a localized lattice disturbance on the chain. Again, since the adiabatic response rate is significantly faster than the transition rates between levels, we expect the resulting lattice distortion to directly reflect the transient distribution of the excited carrier in energy.

This evolution of the bond-alternation profile as the carrier relaxes towards the band edges is displayed more quantitatively in Fig. 3, in which we plot the squares of the amplitudes of the Fourier components of the bond-alternation pattern for three times following photoexcitation of a π electron. The data are averaged on a 20-fs window (a phonon period) centered on the times given in the insets. For the shortest time shown, the distortion is strongly peaked on the Fourier component which is tuned to the photoexcited state through the instantaneous adiabatic force. As time progresses,

this distribution spreads and shifts to lower momenta, in concert with the relaxation of the carrier towards the band edge.

Unfortunately, many of these interesting excited-state phenomena occur extraordinarily rapidly following photoexcitation so that direct experimental study of them may be difficult. However, we do call attention to two important experimental consequences of these results.

The first of these involves secondary-photon emission spectra in $(CH)_x$.[12–15] In a previous Communication[18] we noted a possible connection between the fast excitation-frequency-dependent adiabatic relaxations described here and the unusual Raman line shapes reported in $(CH)_x$; here we develop this idea in more detail. Immediately after the π electron is excited in the polymer, the lattice is driven towards a specific distortion as defined by the adiabatic force in Eq. (7). At longer times the lattice distortion evolves further, as amplitude for the excited electron develops in states closer to the band edge. We now consider a radiative recombination of the electron and hole which occurs during such a relaxation. The radiative decay occurs suddenly with respect to the lattice response time, so that in the familiar Frank-Condon picture, the configuration of the ion coordinates in phase space remains stationary during the deexcitation. We interpret the instantaneous phase-space coordinates[20] (q,p) of the classical system as the expectation values of (q,p) evaluated in a quantum-mechanical

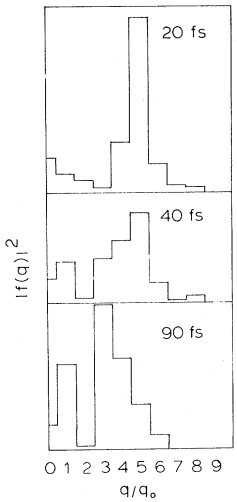

FIG. 3. Momentum distributions for the lattice configurations shown in Fig. 2. The distributions are averaged over a 20-fs window centered on the times given in the insets. Here q_0 is the wave vector of the longest standing wave of chain, i.e., $q_0=2\pi/L$, where L is the chain length.

wave packet for the lattice degrees of freedom.[21] If the atomic displacements from their ground-state equilibrium positions are small compared to the zero-point envelopes for the ion positions, then the expectation values (q,p) can be used to specify the quantum phonon occupation distribution in the recombined state. Thus the occupation probability (number) for a phonon of band index n and wave vector q in the recombined state is

$$p_n(q)=|f_n(q)|^2+|g_n(q)|^2 , \tag{16}$$

where

$$|f_n(q)|^2=\frac{m\omega}{2\hbar}\left|\sum_{j=1}^{N}u_j(t)\xi_j(n,q)\right|^2 \tag{17a}$$

and

$$|g_n(q)^2=\frac{m}{2\hbar\omega}\left|\sum_{j=1}^{N}\dot{u}_j(t)\xi_j(n,q)\right|^2 , \tag{17b}$$

where $\xi_j(n,q)$ is the projection of the mode (n,q) on the jth atom coordinate.[22] This occupation probability corresponds to a probability for leaving the system in a vibrationally excited state after the radiative decay. Energy conservation thus requires that the radiated spectrum contain a Stokes-shifted sideband calculable as a convolution over the distribution function in Eq. (16):

$$I(\omega)=\int\int dt\,dq\,p_n(q,t) \times\delta(\omega-\omega_0+\omega_n(q))e^{-\lambda t} . \tag{18}$$

Here ω_0 is the exciting frequency and the exponential factor in the integrand results from the transient decay of the electron from the original photoexcited state. We have evaluated the line shape given by Eq. (18) by extending our results from the 48-atom chain to an "infinite" chain as follows. We assume that the electrons propagate in a one-dimensional band with dispersion near the zone boundary k_0 given by

$$E(k)=\pm[\Delta^2+h^2v_F^2(k-k_0)^2]^{1/2} , \tag{19}$$

where $\Delta=1$ eV, $k_0=1.3$ Å^{-1}, and $hv_F=7.2$ eV Å.[23] Thus photoexcitation at frequency ω_0 couples valence and conduction states at wave vector k, where

$$k=\pm[\tfrac{1}{4}(\hbar\omega_0)^2-\Delta^2]^{1/2} . \tag{20}$$

The subsequent transient response of the lattice depicted in Fig. 3 is then modeled by fitting those momentum distributions to normalized Lorentzian distributions with a time-dependent peak position

and width chosen to reproduce the time evolution of the distributions shown in the figure. Finally, the phonon dispersion $\omega(q)$ is taken from our previous force-field calculations for the 1450-cm^{-1} band of *trans*-$(CH)_x$.[24] This band is dominantly a bond-length oscillation of the double bonds in the polymer, and its line shapes in the Stokes-shifted spectrum has been the subject of extensive experimental study. The residence time in the initially excited state, $1/\lambda$ in Eq. (8), is taken to be the electron-phonon scattering time, or roughly a phonon period in this system ($\sim$20 fs). The resultant line shapes are plotted for several exciting frequencies ω_0 in Fig. 4. For primary excitation close to the adsorption threshold (2 eV) we obtain a narrow line shape tailing towards higher scattered phonon energy. As the excitation frequency is increased a well-defined second peak develops, again shifted towards higher scattered phonon frequency. The overall width of the Stokes-shifted line reflects the frequency distribution of vibrations driven during the transient response of the polymer backbone to the photoexcited electron. As the primary excitation frequency approaches the optical threshold, the driven vibrations are weighted more strongly towards long wave lengths, causing the Stokes line shapes to narrow.

The line shapes presented in Fig. 4 provide a very satisfactory account of the line shapes experimentally measured in $(CH)_x$ films.[12,24] These unusual line shapes have been commonly observed in resonant Raman-scattering experiments in $(CH)_x$ and have been generally attributed to a resonance effect resulting from a distribution of conjugation lengths in the polymer. Our results suggest that the line-shape variation is indeed a resonance effect, resulting instead from the dynamic response of a long chain to photoexcitation. We have previously anticipated the excitation-frequency dependence of the positions of the shifted peaks shown in Fig. 4 (Ref. 18); however, our present results surprisingly suggest that the position, width of the shifted peak, and the band-edge emission are all dominated by this fast luminescence mechanism in the polymer.[25] Similar results are obtained for all the Raman-active bands in $(CH)_x$ and $(CD)_x$; the overall widths of these lines differ because of the $\omega_n(q)$ contribution to the line shapes in Eq. (18).

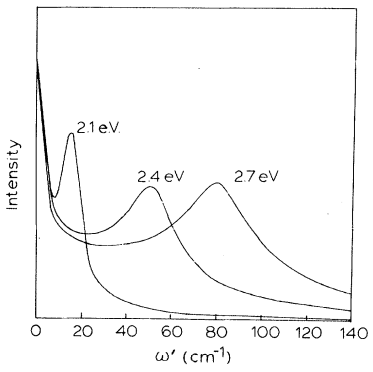

FIG. 4. Line shapes for the Stokes-shifted line corresponding to the C=C stretch in $(CH)_x$. $\omega'=0$ corresponds to the band edge of the Stokes-shifted radiation (experimentally $\sim$1450 cm^{-1}). The inset energies label the primary excitation frequency, ω_0.

This incoherent secondary emission is measurably strong in the inelastic spectrum. The yield for this emission can be estimated straightforwardly from the absorption cross section $\sigma_a(\omega)$ and the radiative and nonradiative relaxation rates. The cross section for secondary emission by luminescence is then

$$\sigma_L(\omega)=\sigma_a(\omega)\tau_{\rm nr}/\tau_{\rm r} . \tag{21}$$

Reasonable estimates are obtained by extracting σ_a from experiments (10×10^{-18} cm^2 to 5×10^{-18} cm^2 within 1 eV of the absorption maximum), $\tau_{\rm nr}$ from our dynamics calculation ($\tau_{\rm nr}\sim$20 fs), and τ_r from the transition probability between valence and conduction eigenstates of the Hamiltonian in Eq. (1) ($\tau_{\rm r}\sim10^{-7}$ s). Thus we estimate $\sigma_L(\omega)\approx2\times10^{-24}$ cm^2. This cross section is large compared to typical Raman cross sections even in a resonance Raman experiment, and furthermore agrees moderately well with recent experimental measurements of the inelastic-light-scattering cross section.[26] We conclude that it is likely that the inelastic-light-scattering spectra observed in this polymer are dominated by this form of incoherent emission. If so, the unusual Stokes-shifted line shape is a direct manifestation of the interesting structural relaxation pathway we have described.

Experiments which could potentially distinguish incoherent and coherent emission would clearly be useful for distinguishing between the homogeneous and inhomogeneous line-broadening mechanisms proposed for this system. An interesting property peculiar to the luminescence model is that the secondary emission can, in principle, be dispersed in time following the photon absorption. To demonstrate this effect, we have decomposed the line shape for $\omega_0=2.7$ eV by limiting the range of the time integration in Eq. (18). The results are displayed in Fig. 5. Here we have calculated the emission over a 50-fs time window following delays of 0, 50, and 125 fs after the primary photon is absorbed. We observe that earliest emission is centered about the corresponding shifted peak in Fig.

4. As the relaxation proceeds the emission becomes more strongly weighted towards the phonon band edge.

A second experimental consequence of these dynamic studies to which we call attention involves the time required to ultimately generate solitons after photoexcitation. Our results are consistent with previous dynamics studies which indicate that the time required to geminate these defects is extraordinarily short if the system is prepared with the photoexcited carriers at the band edge.[11] Unfortunately, the typical experimentally realized situation excites the carriers 0.2—1.0 eV above the band edge. In this experimental situation the creation of these photogenerated defects is ultimately limited by the time required for the carrier to relax to the band edge, which is apparently substantially longer than the "adiabatic" time. Over the longest intervals studied in the present calculation (0.5 ps) the carrier is continuing to relax towards band-edge states; it is likely that the full relaxation requires times on the order of, but exceeding, 1 ps. As we have seen, this relaxation proceeds by an interesting pathway characterized by a continuous evolution and growth of the bond-alternation defects as the carrier relaxes. This suggests that some of the later stages of this relaxation can be directly probed experimentally in time-resolved measurements.

In summary, we have developed a scheme to directly study vibrational intramolecular relaxation in a complicated polyatomic molecule and have applied it to study structural relaxation following photoexcitation in a long polyene. We find that the early stages of this relaxation are dominantly describable in terms of an adiabatic relaxation on a single excited-state surface. For longer times nonadiabatic processes dominate the relaxation, and the evolution of the excited electron between excited states is reflected in the transient distortions exhibited by the bond-alternation profile on the polyene. The bond-alternation pattern undergoes a series of bounces, from which photogenerated solitons ultimately emerge. Radiative decay from the molecules undergoing such a relaxation will exhibit a Stokes-shifted sideband with a line shape which depends sensitively on the primary excitation frequency. Finally, since the nonadiabatic aspects of this relaxation are the time-limiting step in the relaxation of such excited molecules, the gemination of solitons following photoexcitation may extend into a time regime in which it can be directly monitored experimentally.

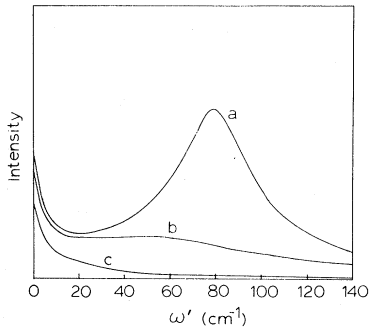

FIG. 5. Time dispersion of the Stokes-shifted line for 2.7-eV primary excitation shown in Fig. 4. The data are averaged over a 50-fs window following delays of (a) 0 fs, (b) 50 fs, and 125 fs after photoexcitation.

Helpful discussions with D. P. DiVincenzo are gratefully acknowledged. This work was supported in part by the National Science Foundation—Materials Research Laboratory (NSF-MRL) program under Grant No. DMR-7923647 and NSF Grant No. DMR 82-03484.

[1]C. K. Chiang, C. R. Fincher, Y. W. Park, A. J. Heeger, H. Shirikawa, E. J. Louis, S. C. Gau, and A. G. MacDiarmid, Phys. Rev. Lett. 39, 1098 (1977).

[2]C. K. Chiang, S. C. Gau, C. R. Fincher, Y. W. Park, A. G. MacDiarmid, and A. J. Heeger, Appl. Phys. Lett. 33, 18 (1978).

[3]K. Kaneto, M. Maxfield, D. P. Nairns, A. G. MacDiarmid, and A. J. Heeger, J. Chem. Soc. Faraday Trans. (in press).

[4]M. J. Rice, Phys. Lett. 71A, 152 (1979).

[5]W. P. Su, J. R. Schrieffer, and A. J. Heeger, Phys. Rev. Lett. 42, 1698 (1979).

[6]B. R. Weinberger, J. Kaufer, A. J. Heeger, A. Pron, and A. G. MacDiarmid, Phys. Rev. B 20, 2231 (1979).

[7]C. R. Fincher, M. Ozaki, A. J. Heeger, and A. G. MacDiarmid, Phys. Rev. B 19, 4140 (1979).

[8]N. Suzuki, M. Ozaki, A. J. Heeger, and A. G. MacDiarmid, Phys. Rev. Lett. 45, 1209 (1980); 45, 1463 (1980).

[9]E. J. Mele and M. J. Rice, Phys. Rev. Lett. 45, 926 (1980).

[10]S. Etemad, A. Pron, A. J. Heeger, A. G. MacDiarmid, E. J. Mele, and M. J. Rice, Phys. Rev. B 23, 5137 (1981).

[11]W. P. Su and J. R. Schrieffer, Proc. Nat. Acad. Sci., U. S. A. 77, 5626 (1980).

[12]L. S. Lichtmann, A. Sarhangi, and D. B. Fitchen, Solid State Commun. 36, 869 (1981).

[13]H. Kuzmany, Phys. Status Solidi 97, 521 (1980).

[14]D. B. Fitchen, Mol. Crys. Liq. Crys. (in press).
[15]L. Lauchlan, S. Etemad, T.-C. Chung, A. J. Heeger, and A. G. MacDiarmid, Phys. Rev. B 24, 3701 (1981).
[16]J. Orenstein and G. L. Baker (unpublished).
[17]D. Vanderbilt and E. J. Mele, Phys. Rev. B 22, 3939 (1980).
[18]E. J. Mele, Solid State Commun. (in press).
[19]N. Bloembergen, *Nonlinear Optics* (Benjamin, New York, 1956).
[20]Here q and p are vectors in 48-dimensional spaces spanning the structural degrees of freedom of the polyene.
[21]Thus the time evolution of the quantum expectation values is replaced by the evolution of the classical coordinates which should be an excellent approximation in this 48-dimensional space.
[22]Outside the small displacement regime,

$$p=(|f|^2+|g|^2)\exp[-(|f|^2+|g|^2)] .$$

[23]This produces a peak in $\epsilon_2(\omega)$ at 2.0 eV, near the where the peak is experimentally observed in Ref. 8.
[24]E. J. Mele, Mol. Crys. Liq. Crys. 77, 25 (1981).
[25]L. S. Lichtmann, Ph.D. thesis, Cornell University, 1981 (unpublished).
[26]The peak scattering cross section in *trans*-$(CH)_x$ has been recently measured yielding $\sigma\sim 3\times 10^{-24}$ by L. Lauchlan (private communication and unpublished).